Surface Science 272 (1992) 118–129
North-Holland

surface science

Probing surfaces with thermal energy atoms: proposal for a novel triple-axis He–surface spectrometer

Klaus Kuhnke [a,b], Elmar Hahn [a,b], Rudolf David [b], Peter Zeppenfeld [b] and Klaus Kern [a,b]

[a] *Institut de Physique Expérimentale, EPF-Lausanne, PHB-Ecublens, CH-1015 Lausanne, Switzerland*
[b] *Institut für Grenzflächenforschung und Vakuumphysik, KFA-Forschungszentrum Jülich, Postfach 1913, D-5170 Jülich, Germany*

Received 12 November 1991; accepted for publication 20 January 1992

The basic principals of thermal energy atom scattering from surfaces are discussed. The performance and limitation of modern He–surface scattering spectrometers are analyzed. In analogy to the classical double surface scattering experiment of Estermann, Frisch and Stern for selecting and detecting the velocity of a beam of thermal atoms, it is proposed to use double surface scattering to build a triple-axis He–surface spectrometer. Regularly stepped metal surfaces as monochromator- and analyzer-crystal turn out to be the clue for a superior energy resolution and dynamical range.

1. Helium–surface scattering

A general approach to obtain the static and dynamic properties of solid surfaces is a scattering experiment. An incoming beam of probe particles (e.g. electrons, photons, neutrons or atoms) of defined wavevector k_i and energy E_i, impinges on a surface, and the scattered intensity at wavevector k_f and energy E_f is measured in the solid angle element $\delta\Omega$. The complete information which can be deduced in such a scattering experiment, i.e., the behavior of the surface atoms in space and time, is contained in the double differential cross section:

$$\delta Z = I_0 \frac{d^2\sigma}{d\Omega dE_f} \delta\Omega \delta E_f \qquad (1)$$

where δZ is the number of probe particles in the energy interval δE_f scattered into the solid angle element $\delta\Omega$, and I_0 the intensity of the incoming probe particles. Except for trivial factors, the scattering cross section is determined by the energy exchange ($\hbar\omega$) and the momentum exchange (Q).

$$\frac{d^2\sigma}{d\Omega\, dE_f} \simeq S(Q, \hbar\omega),$$
$$\hbar\omega = E_f - E_i,\ Q = k_f - k_i. \qquad (2)$$

The selection of the probe particles is determined by the characteristic energy, time and length scales of the surface phenomena to be investigated. In fig. 1 we have indicated characteristic energies of collective surface excitations and important length scales by the hatched regions. In order to gain information on the different processes in a surface scattering experiment it is favorable when energy and momentum of the probe particles simultaneously match the characteristic parameters of the surface phenomena (energy, $\hbar\omega$; time, $1/\omega$; and length, $1/Q$). In order to visualize this correlation we have included in fig. 1 the wavelength-energy dispersion for the different probe particles. Obviously, the λ-$\hbar\omega$ range accessible to the electrons, neutrons and atoms (here He-atoms), coincides with the energy and time-scales which are characteristic for collective excitations and atomic movements on the surface. On the other hand, for electromagnetic waves this coincidence is absent, generally $\hbar\omega$ and Q do not match.

The matching of the particle wavelength with typical interatomic distances of surfaces which can be achieved for all probe particles in fig. 1 gives rise to interference effects in the scattering and can be detected by scanning the scattering angle or the wavelength. In such a diffraction

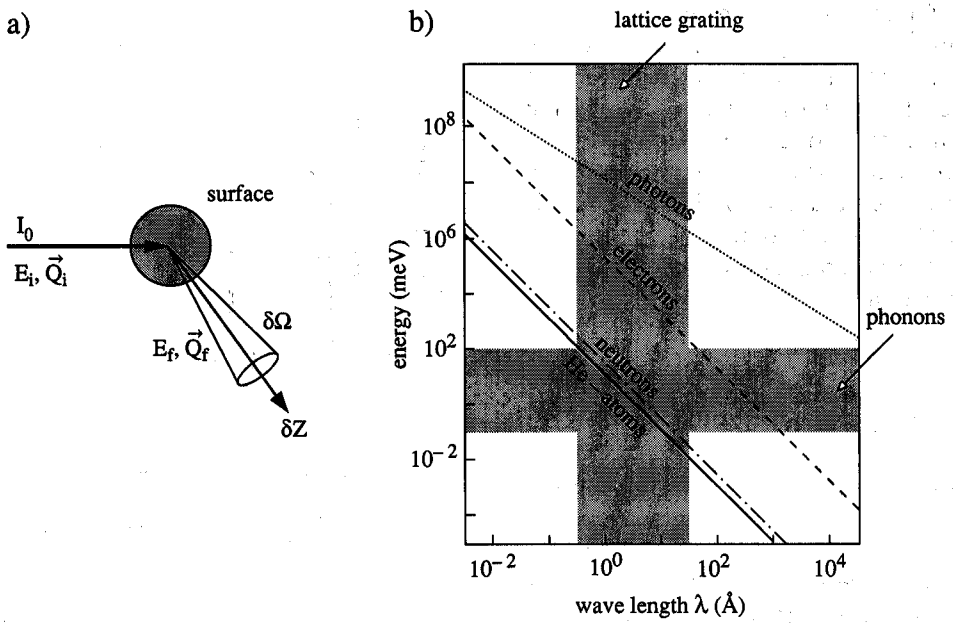

Fig. 1. (a) Sketch of a surface scattering experiment. (b) Wavelength-energy dispersion of electrons, neutrons, He-atoms and phonons. The hatched regions indicate characteristic energy ranges of collective surface excitations and typical length scales.

experiment no energy analysis is usually done, i.e., the differential cross section $d\sigma/d\Omega$ is measured. Diffraction is still the dominating tool in determining surface structures, even in the age of STM. Historically, it was indeed surface diffraction by which de Broglie's hypothesis of the particle-wave dualism has been proven more than 60 years ago. In a beautiful set of experiments Davison and Germer [1] and Stern, and co-workers [2] demonstrated the reality of de Broglie waves associated with material particles by detecting diffraction signatures in the scattering of electrons and thermal He-atoms from a Ni(100) and a LiF(001) surface, respectively.

The most stringent requirement for probe particles when used in studies of surfaces, however, is an adequate surface sensitivity. From this point of view, thermal atoms are the most appropriate probe particles. Because of their large cross section, thermal atoms of small energy (< 100 meV) interact with the outermost layer only; there is no penetration into deeper layers. The classical turning point of thermal energy atoms is usually a few ångström above the ion cores of the outermost layer.

It is the exclusive surface sensitivity of thermal atom scattering in combination with the unique $\hbar\omega - Q$ matching which makes this method an outstanding surface probe. This was recognized more than sixty years ago by T.H. Johnson [3]: *"These experiments are of interest not only because of their confirmation of the predictions of quantum mechanics, but also because they introduce the possibility of applying atom diffraction to investigations of the atomic constitution of surfaces. A beam of atomic hydrogen, for example, with ordinary thermal velocities, has a range of wavelengths of the right magnitude for this purpose, centering around 1 Å, and the complete absence of penetration of these waves will insure that the effects observed arise entirely from the outermost atomic layer."*

Today, thermal energy atom scattering is one of the most sensitive means to examine surface structure [4], to learn about surface motions [5], surface phase transitions [6], surface growth [7],

etc. The preferred probe atom, however, is not hydrogen but ^{4}He. High-pressure nozzle expansions of He provide atomic beams with high intensities and the sharpest velocity distributions [8]. Indeed, intensities of 10^{19} He-atoms s^{-1} sr^{-1} and monochromaticities of $\Delta v/v = \Delta\lambda/\lambda = \Delta E/2E \approx 0.01$ are obtained routinely today. The inert nature of He in addition ensures that thermal energy He scattering is a completely nondestructive surface probe.

2. Performance and limitations of He time-of-flight spectrometers

Fig. 2 shows schematically a He-atom–surface scattering experiment. A highly monochromatic beam of thermal He-atoms ($\Delta\lambda/\lambda \leq 1\%$) is generated in a high pressure supersonic expansion and collimated to a few tenths of a degree by a series of specially shaped collimators, so called skimmers. Depending on the source temperature, the wavelength of the He-atoms ranges between 0.3 and 2.0 Å; typical fluxes are of the order 10^{19} He atoms/s sr. The He-atoms scattered from the crystal surface into a well defined solid angle elements Ω are detected by an electron impact ionization mass spectrometer. The scattered intensity can be either measured energy integrated or energy resolved. In the latter case, the scattered beam is divided into pulses by a chopper

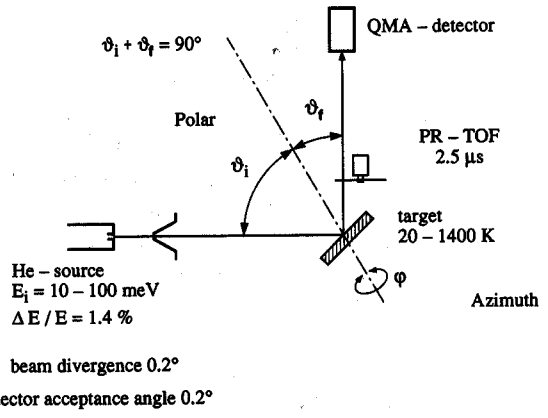

Fig. 2. Schematic arrangement of a He–surface scattering experiment.

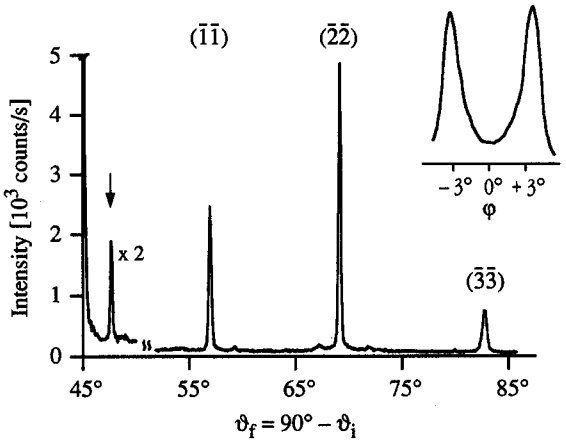

Fig. 3. Polar and azimuthal (inset) He-diffraction scan of a complete Xe-monolayer on Pt(111); He wavelength λ_{He} = 1.098 Å, surface temperature T = 25 K.

and the times of arrival of He-atoms at the detector are analyzed. Since the initial energy of the He-atoms and the geometry of the experiment are known, the energy transfer during the scattering can be calculated. For experimental details of a typical spectrometer we refer the reader to ref. [9].

In contrast to electron spectrometers, where either the elastic or the inelastic scattering cross-section are measured in order to obtain structural information (LEED) or dynamical information (EELS), respectively, the currently operated high resolution He scattering spectrometers are hybrids. They are designed to measure structural and dynamical surface properties in one experiment, i.e., designed to measure the double differential scattering cross-section. This duality is usually achieved at the expense of very high diffraction capabilities.

The performance of a highly-advanced He time-of-flight spectrometer (HETOF-1 [9]) is demonstrated in figs. 3 and 4.

In fig. 3 we show as an example a He-diffraction scan from a complete Xe-monolayer adsorbed on Pt (111) ($\theta_{Xe} \approx 0.42$ Xe-atoms per Pt substrate atoms); a well behaved diffraction pattern with sharp Bragg-peaks is observed. This diffraction scan has been measured in a fixed scattering geometry $\vartheta_f + \vartheta_i = 90°$ by rotating the

Pt-crystal around an axis perpendicular to the scattering plane; the angle on the abscissae scales to a parallel momentum transfer scale by the relation $Q'' = 5.723(\sin\vartheta_f - \cos\vartheta_f)$. The diffraction pattern characterizes a hexagonal densely packed 2D-Xe crystalline solid with a nearest-neighbor distance of 4.33 Å. In the inset of fig. 3 the orientational structure (with respect to the Pt-substrate) of the Xe-monolayer is characterized in an azimuthal diffraction profile, which is obtained by rotating the Pt-crystal around its surface normal at a fixed polar angle corresponding to a Bragg-position. The symmetric peak-doublet centered along the $\overline{\Gamma}\overline{K}_{Pt}$ direction of the substrate surface characterizes a Novaco–McTague phase rotated $\pm 3.3°$ degrees off the natural R30° orientation of submonolayer Xe-films (see ref. [10]).

In an energy resolved scattering experiment, from the measured He-energy loss ($\Delta E < 0$) or gain ($\Delta E > 0$) the phonon energy $\hbar\omega$ and the corresponding phonon wavevector Q'' parallel to the surface is straightforwardly determined from the conservation of energy $\Delta E = E_f - E_i = \hbar\omega$ and parallel wavevector $\Delta K = K_f - K_i = Q''$. In the case of in plane scattering the relation between energy and momentum transfer is then given by the scancurve

$$\Delta E = E_i\left[\left(\frac{\sin\vartheta_i + \Delta K/k_i}{\sin\vartheta_f}\right)^2 - 1\right], \qquad (3)$$

where $k_i = \sqrt{2m_{He}E_i}/\hbar$ denotes the wavevector of the incoming He-atoms. As an example, fig. 4 shows an inelastic He scattering spectrum from the same monolayer of Xe on Pt (111) obtained with a primary He-beam energy of 18.3 meV at a scattering angle $\vartheta_i = 90° - \vartheta_f = 38°$ along the $\overline{\Gamma}\overline{K}$ symmetry direction of the Xe-layer [11]. The small peak at zero energy transfer represents the purely elastically scattered He atoms. Away from the position of the Bragg-peaks of the overlayer, the intensity of this diffuse elastic peak is a sensitive measure of the perfection and cleanliness of the surface. The main peak at -3.35 meV ($Q'' = 0.57$ Å^{-1}) corresponds to the creation of a Xe-monolayer phonon associated with the vertical Xe–Pt vibration.

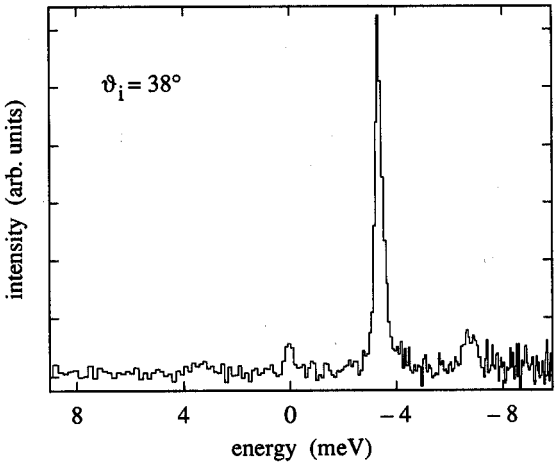

Fig. 4. He TOF spectrum (transferred to an energy scale) of a Xe-monolayer on Pt(111) taken at an angle of incidence $\vartheta_i = 90° - \vartheta_f = 38°$; primary He-beam energy $E_i = 18.3$ meV, surface temperature $T = 25$ K.

The figures of merit characterizing the performance of a hybrid He TOF-spectrometer are the transfer-width and the energy resolution. The transfer-width [12] which is a measure of the momentum resolution in diffraction is determined by the angular opening of the He-beam and of the detector and by the monochromaticity of the He-wave. The instrument HETOF-1, designed to measure structural and dynamical surface properties in the same experiment, which is achieved at the expense of high-diffraction capabilities, has a transfer width of about 400 Å for a 18 meV beam at specular ($\vartheta_i = \vartheta_f = 45°$) geometry.

The effective energy resolution of the TOF-spectrometer is determined by four contributions: the effective resolution function of the chopper (taking into account the finite width of the beam, of the chopper slots and of the channels), the monochromaticity of the He-beam, the finite length of the detector ionization region and of course the length of the flight path. The TOF-spectrum with the highest resolution measured so far is the spectrum in fig. 4 and its cousins reported in refs. [13,14]. The energy width of the Xe-loss peak (purely determined by instrumental factors) is $\Delta E = 0.32$ meV (FWHM) at a primary energy of 18.3 meV resulting in $\Delta E/E = 0.017$. A

figure of comparable quality $\Delta E/E = 0.022$ has been reported by Eichenauer et al. [15] for Cu (111) phonon inelastic peaks.

The significant improvement of the transfer-width and the energy resolution, say by one order of magnitude, would require a simultaneous improvement in all the contributions mentioned above. While the angular openings of He-beam and detector can easily be reduced and the influence of the finite ionization region can be diminished by increasing the flight path (all of course at the expense of beam intensity), neither the effective resolution function of the chopper nor the monochromaticity of the He-beam can be increased arbitrarily.

The improvement of the chopper resolution is constrained by the mechanical strength of the chopper blade: at a constant chopper frequency the increase of resolution would require the decrease in the slit width, which however requires a thinning of the chopper blade in order to ensure sufficient transmission. With current technologies it seems to be hardly possible to drop the chopper resolution function below about 1 μs (2.5 μs currently in the HETOF-1 instrument).

An increase in the monochromaticity of the primary He-beam is even more difficult to achieve. Energy half widths (FWHM) of $\Delta E/E \cong 0.015$ in the beam are obtained in continuous nozzle beam sources today. A decrease beyond a factor of 2 by increasing source pressure and/or nozzle diameter would require enormous pumping capabilities in the source region and might at low source temperatures even be prevented by the onset of cluster formation in the beam [16]. Pulsed sources which have proven to be successful at room temperature [17] suffer from the low duty cycle and the limited temperature variability.

Thus an improvement in the beam energy resolution requires some active means to skim a selected energy interval out of the energy distribution of the nozzle beam. One obvious way would be the use of a Fizeau-selector. A detailed analysis [18] shows, however, that a velocity selector with the desired energy resolution of $\Delta E/E = 0.002$ has substantial drawbacks. A thin blade selector would require a length of more than 1 m, while a thick-blade selector can be as short as 10 cm but at a price of a transmission coefficient which is only a few permille. A more appealing concept of active monochromatization turns out to be the use of solid surfaces as grating monochromators and will be discussed in the next paragraph.

3. He–surface triple-axis spectrometry

3.1. Monochromatization by diffraction

The active monochromatization of a He-beam was first introduced in 1932 by Estermann et al. [19]. In their beautiful study, the earlier diffraction experiments with effusive He-beams [21] (Maxwellian velocity distribution) from LiF surfaces were refined by the use of monochromatized beams in order to obtain sharper diffraction peaks. Monochromatization was done in two ways. Using a velocity selector consisting of a concentric pair of rotating chopper wheels they narrowed the "Maxwellian" He-beam down to a few percent. Using these beams allowed the authors to verify the de Broglie relation $\lambda = h/mv$ with an accuracy of about 1%.

The second concept of monochromatization by diffraction from a crystal surface (LiF in their experiment) and selection of atoms within a narrow range of diffraction angles is even more appealing. The scheme of this experiment is shown in fig. 5. An effusive He-beam is first scattered off one LiF(001) surface; the diffracted beam is selected in direction and the aperture prepares an energy selected He-beam from the impinging Maxwellian distribution. The second LiF surface than analyzes the monochromaticity of the prepared energy distribution by recording the resulting diffraction pattern. The success of the monochromatization technique is demonstrated in the right part of fig. 5. In enjoying this experiment the reader should keep in mind that it has been carried out sixty years ago, long before ultra-high vacuum conditions could be achieved or measured. It is instructive to study the original manuscript with its technical details to fully appreciate the brilliant experimental achievements of Stern and co-workers.

Basically the arrangement in fig. 5 already contains the ingredients of a He–surface triple- or double-axis spectrometer; the surface to be investigated has just to be added between the aperture and the analyzer crystal and the necessary rotational degrees of freedom in the scattering plane have to be provided. In such a crystal spectrometer, the total experimental energy resolution which can be achieved is solely determined by geometrical parameters, in particular by the angular opening of beam and detector and the size of the monochromatizing aperture. By shrinking the aperture and the angular openings the resolution can theoretically be made arbitrarily good (for a parallel beam!). Practically this resolution tuning is however limited by the low detection sensitivity of usual He-detectors (10^{-5}–10^{-6}), which require a significant He-beam intensity and by the finite divergence of the He-beam (see section 3.2).

Energy-resolution limitations due to He-flux problems are indeed severe when using surfaces like LiF(001) as monochromator and analyzer. Out of the impinging He-flux on the monochromator surface, only that part which is diffracted in the selected diffraction order is of further use and even this part of the intensity will be further reduced by the monochromatizing aperture according to the selected energy resolution. Due to the large corrugation of the alkali halide surfaces, however, numerous intense in-plane and out-of-plane diffraction peaks are present [20]. But only one of them is selected for further monochromatization; which represents hardly more than 1% of the incoming flux. Assuming a monochromatization by one order of magnitude (from $\Delta E/E = 0.02$ of the incoming He nozzle beam to $\Delta E/E = 0.002$) less than 1 permille of the incoming particle flux survives, i.e., impinges on the surface to be investigated. The same percentage is again lost by analyzing the surface scattering with the LiF analyzer crystal.

Mason and Williams [21] in 1978 have built a He-surface double-axis spectrometer by using a LiF(001)-surface as analyzer crystal but omitting a monochromator crystal. The resolution of this spectrometer was reported to be $\Delta E/E \cong 0.043$ at a primary energy of 23 meV [22], i.e., about a factor of 2 worse than the best TOF-spectrometers.

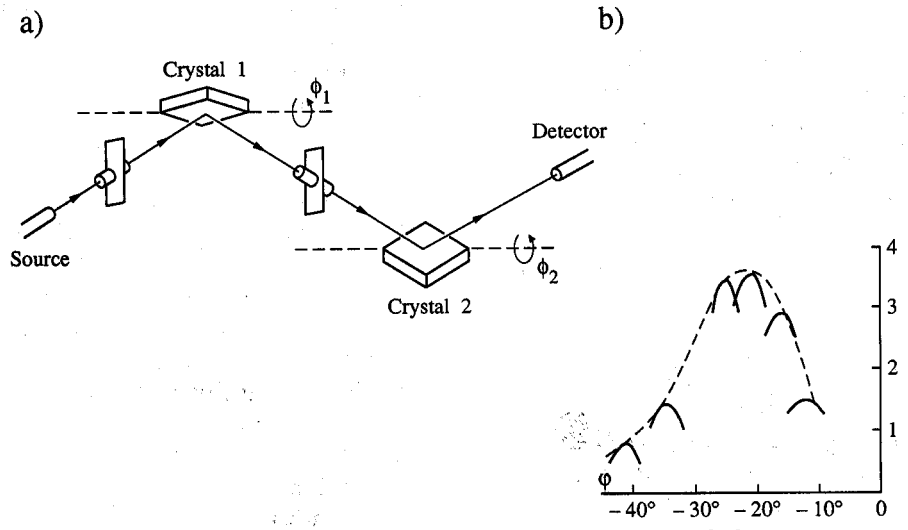

Fig. 5. (a) Schematic view of the double surface scattering experiment of Estermann et al. [19]; the two LiF crystals can be tilted while the two apertures are fixed. (b) First-order diffraction peak of the analyzer crystal at different settings of the monochromator crystal (fat line). The monochromatization with respect to the Maxwellian diffraction (dashed line) is obvious.

3.2. The microscopic Echelette-grating for He-waves

In the last paragraph we have demonstrated that we run into severe intensity problems when using alkali halide surfaces as grating monochromators or analyzers. In the following section we will demonstrate an elegant alternative which allows monochromatization of a He-beam without excessive intensity losses.

In classical optics the so-called Echelette-gratings introduced in 1910 by R. Wood are well known. These are stepped reflection gratings which for well defined step arrangements (the periodic step distance is of the order of the wavelength of the reflecting light and much larger than the step height) reflect almost the total incoming intensity in one higher diffraction order. But can nature provide us with Echelette-gratings also for He-waves (typical wavelengths between 0.5 and 2.0 Å)? Such a grating would have to feature highly reflecting flat regions separated by regularly spaced steps, several ångström apart and about 1 Å in height.

There exists a class of surfaces, the close packed (111) fcc metal surfaces like Pt(111), which indeed act as mirror for thermal He-atoms [23].

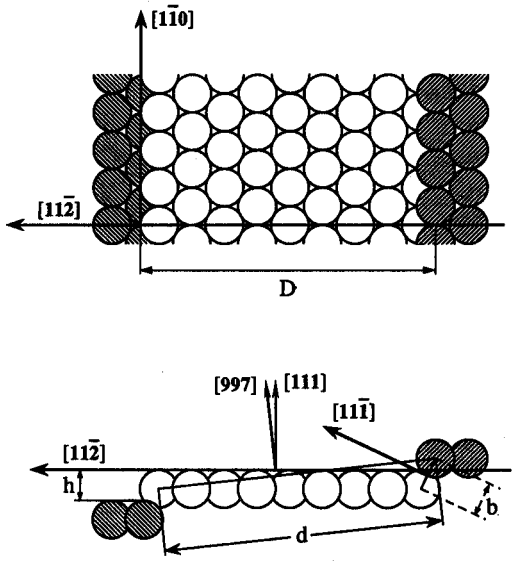

Fig. 6. Echelette-grating for He-waves : side and plane view of a Pt(997) surface; $d = 20.2$ Å, $h = 2.27$ Å.

In a well prepared state these surfaces can reflect more than 60% of the incoming intensity in the specular direction. Moreover, by cuting a surface with an angle α slightly misoriented with respect to the (111) face one obtains a surface which exhibits all the properties of an Echelette-grating for He-waves. An example is the Pt(997) surface shown in fig. 6. This is a regularly stepped surface consisting of (111) terraces, separated by monatomic steps.

The He-diffraction from such a surface is described by the product of a structure function and a form factor function:

$$I \propto A^2 G^2. \tag{4}$$

The form factor A^2 is determined by scattering from the unit cell (terrace mirror) and is also called envelope function. In the plane wave approximation it corresponds to the well known result of slit diffraction in optics:

$$A^2 = \frac{\sin^2(\phi/2)}{(\phi/2)^2}, \tag{5}$$

$$\phi = \frac{2\pi}{\lambda}\tilde{D}[\sin(\vartheta_i - \alpha) - \sin(\vartheta_f + \alpha)],$$

$$\tilde{D} = D(1 - \tan\alpha \tan(\vartheta_i - \alpha)).$$

Here, $\tilde{D}$ accounts for the fact that the He-wave sees only an effective terrace length due to the shadowing of the step edge.

The structure function G^2 describes the interference between terraces and is given by

$$G^2 = \delta(\sin\vartheta_f - \sin\vartheta_i - n\lambda/d). \tag{6}$$

For each angle of incidence the positions of the diffracted beams are given by the structure function (6); its height is determined by the envelope function (5). Variation of the angle of incidence leads to a continuous shift of the positions of the diffracted beams with respect to the specular direction to the terraces. Since the specular direction to the terraces and the macroscopic one are separated by an angle 2α, the diffracted beams of a certain order n can be made to coincide with the specular direction to the terraces, by a suitable choice of the angle of incidence, i.e., the reflected beam intensity can be

concentrated in one single high-order diffraction peak. This behavior is illustrated in fig. 7 showing He-diffraction patterns from Pt(997) measured by Comsa et al. [24] more than ten years ago.

The Pt(997) surface acts as an Echelette-grating for He-waves. When using this surface as grating monochromator or analyzer only those He-atoms are cut out of the beam which have the "wrong" energy. For a parallel beam of He-atoms the energy spread can be made arbitrarily small by adjusting of the monochromatizing aperture skimming the high-order reflection. In reality, however, the incoming He-beam has a finite angular divergence and the variation of the angles of incidence smears out the dispersive wavelength separation of the Echelette. Taking into account the finite beam divergence δ_{He} the resolving power of the Pt(997) surface can be calculated to be [25]

$$\frac{\Delta E}{E} \gtrsim \frac{D}{h}\delta_{He}, \tag{7}$$

for scattering in step down direction. The maximum achievable energy resolution thus directly relates to the divergence of the incoming He-beam. For the Pt(997) surface an energy resolution of $\Delta E/E = 0.002$ would require a beam angle spread as low as 0.012°.

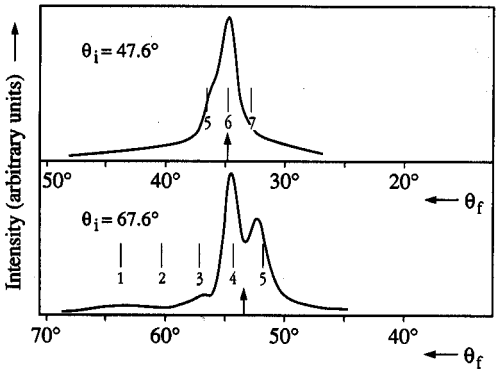

Fig. 7. Experimental He-diffraction pattern of a flat Pt(997) surface measured by Comsa et al. [24] for two different angles of incidence. The He-energy was $E = 63$ meV. The residual intensities in the 5th and 7th diffraction order of the upper scan are due to the poor energy resolution of the primary He-beam which was only $\Delta E/E \approx 0.10$.

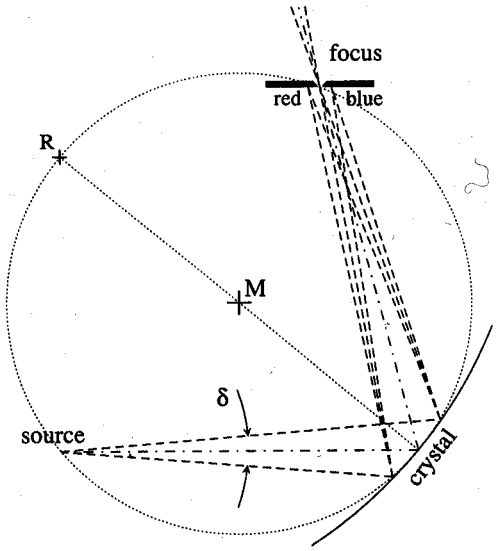

Fig. 8. Rowland-construction for a dispersive wavelength separation by diffraction from a concave Pt(997) surface. A He-source emits a He-beam of divergence δ_{He} which after reflection from a concave Pt(997) surface is focused on the Rowland circle. The path length difference of beams which are reflected at different microscopic terraces results in a spectral dispersion of the beam in the focus. He-source, crystal and focus are located on a circle centered at M; the center of the radius of curvature of the Pt(997) crystal is R. The beam divergence has been exagerated.

3.3. Compensation of the dispersion smearing by focussing

For a plane Echelette-grating the envisaged energy resolution of 2 permille can only be achieved by reducing the beam divergence from currently 0.2° to 0.012°, resulting in a loss of intensity of one order of magnitude. This substantial loss of intensity could be avoided by using a concave reflection grating, where the curvature of the crystal surface counterbalances the spread in the angles of incidence. In addition such a concave crystal would focus the divergent He-beam. The technique of monochromatization by diffraction from concave reflection gratings is well established in X-ray crystallography and the geometry of general applicability is the so-called Rowland-construction [26]. In this geometry the radius of curvature of the concave grating equals the diameter of the Rowland circle (see fig. 8). If

the He-source and the concave grating are located on the Rowland circle the wavelengths of the diffracted wave are spatially separated in the focal point, which also is located on the Rowland-circle. Placing an aperture at this point on the Rowland-circle allows the monochromatization of the diffracted beam, down to any precision (only limited by the finite size of the He-source which is several tens of a micron) without any unnecessary loss of intensity.

Using a diameter of 800 mm for the Rowland-circle the insertion of an aperture of 0.1 mm width would result in a monochromatization down to $\Delta E/E = 0.002$ after diffraction from the concave Pt(997) surface. In fig. 9 we show a numerical simulation of the wavelength separation, here for wavelengths of $\lambda_1 = 0.547$ Å (crosses) and $\lambda_2 = 0.54645$ Å (stars) after diffraction from a concave Pt(779) surface. The (779) surface is closely related to the (997) surface; it likewise has (111) terraces but [100] steps instead of [111] steps resulting in a slightly lower value of $d =$ 18.06 Å. The Rowland diameter is 790 mm; the incident angle has been chosen to be $\vartheta_i = 50.7°$ and the selected diffraction order giving full specular reflectivity is $n = 6$ ($\vartheta_f = 36.7°$). The clean wavelength separation in the focal point, situated 633 mm upstream the Pt(779) surface, is obvious, while only 200 mm upstream the Echelette no separation is achieved as expected.

The question which naturally arises as a consequence of the above discussion is the question of the experimental feasibility of a concave Pt(997) surface, or more generally the feasibility of bent single crystal metal surfaces. Indeed, Doak has recently been successful in focussing an He-atomic beam by means of a bent-crystal mirror [27]. The mirror was made of a thin (111) Au film deposited onto a mica substrate which was bent than in situ to form a cylindrical mirror. The reflectivity of these mirrors was about 10% and focussing by a factor of 4 was demonstrated. Udo Linke at the Institut für Grenzflächenforschung und Vakuumphysik at KFA Jülich recently succeeded in preparing Ni and Pt single-crystals with (100) and (997) surface orientations (oriented to better than 0.1°), respectively, as thin as 0.2 mm. These crystals can be nicely bent mechanically or even just by using electrostatic forces [28]. A beautiful example of the use of thin single crystals is given in this proceeding in the article by Sander and Ibach who determined the adsorbate induced stress on Ni(100) by direct observation of the accompanying crystal deformation [29]. We

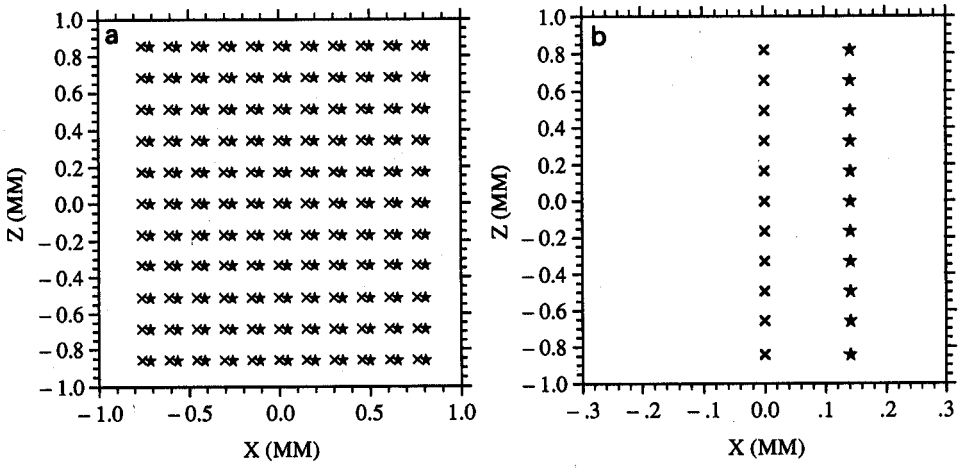

Fig. 9. Numerical simulation of the wavelength separation by specular diffraction from a concave Pt(779) surface. (a) Two beams with wavelengths $\lambda_1 = 0.547$ Å (crosses) and $\lambda_2 = 0.54645$ Å (stars) after diffraction from a concave crystal with curvature 790 mm, 200 mm upstream the crystal center. (b) The same beams at the focus, 633 mm upstream the crystal. The two wavelengths are separated by 0.15 mm.

are currently experimenting with the thin Pt(997) crystal in order to develop a reliable and precisely adjustable crystal bender.

4. Discussion and conclusions

In the present paper we have demonstrated that a triple-axis He–surface spectrometer may feature substantial improvements in the transfer width and the energy-resolution compared to the most advanced He time-of-flight spectrometers. The clue to the higher performance are the use of microscopic Echelette-gratings, i.e., regularly stepped metal surfaces with close packed highly reflecting terraces like the Pt(997) surface. The energy resolution of flat Pt(997) crystals is determined by the finite divergence of the primary He-beam. The divergence smearing can, however, be compensated completely by bending the Pt(997) surface. A concave Pt(997) grating is a perfect He-monochromator or analyzer with minimized intensity losses. Monochromatizing a primary He-beam of $\Delta E/E = 0.02$ by one order of magnitude may result in an intensity loss of less than a factor 20.

There are two aspects which need, however, further consideration in order to evaluate the chances for an experimental realization of such a spectrometer: (1) the influence of irregularities in the periodic step arrangements of the Pt(997) surface which might be in particular important for the bent crystals [30] and (2) the passivation of the Pt(997) surface for a long-term reliable use.

For wavelengths which are scattered in in-phase geometry from the Pt(997) surface, the path length difference from adjacent terraces $\Delta p = h(\cos\vartheta_i + \cos\vartheta_f)$ is independent of the actual terrace width; a finite terrace width distribution thus does not give rise to a broadening of the diffraction peaks. Using the Pt(997) as monochromator or analyzer, however, the wavelength separation capability is the primary figure of interest and we have to investigate the scattering of He-waves which are reflected by the terraces in a slightly nonspecular direction. We have made an analytical ansatz assuming monoatomic steps and a Gaussian distribution of terrace widths [25].

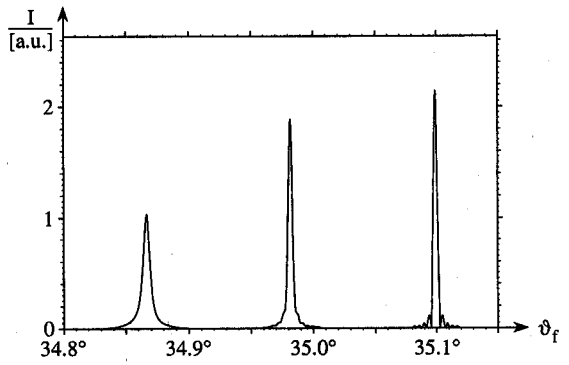

Fig. 10. Broadening of the 6th-order diffraction due to a stochastic distribution of terrace widths of Pt(997). Result of an analytic calculation for two wavelengths $\lambda = 0.5776$ Å (left) and $\lambda = 0.5720$ Å (middle), which deviate from the exact in-phase wavelength $\lambda = 0.5663$ Å (right) by 1% and 2% respectively. The standard deviation of the terrace width distribution was $\sigma_D = 7$ Å; angle of incidence $\vartheta_i = 48.0°$; step height $h = 2.27$ Å; number of interfering terraces $N = 500$.

The terraces are assumed to be point scatters, which does not result in correct intensities (envelope) but generates the Bragg-peak widths accurately. In fig. 10 we show the result of this calculation for three wavelengths, one of which scatters exactly in-phase and two of which are slightly out-of-phase. The terrace width distribution is assumed to be Gaussian with a standard deviation of $\sigma_D = 7$ Å. It is evident that the Bragg reflexes (here the order $n = 6$) are negligibly broadened compared to their relative (wavelength separating) distance. Thus, a moderate mean variation of the terrace width would still allow the use of a Pt(997) surface as He-monochromator or -analyzer.

A reliable use of the Pt(997) as Echelette-grating for He-waves would require that the surface could be made inert to the ambient atmosphere (10^{-10} mbar) in order to ensure a maintenance-free operation for several hours or even days. Such a passivation can indeed be achieved by covering the Pt(997) surface with a full monolayer of hydrogen, which does not influence the step structure and makes the surface highly inert with respect to ambient gases like CO or others [31]. By keeping the passivated Pt-crystal in a continuous hydrogen background atmosphere ($\sim 10^{-8}$

mbar) the surface can be kept clean over several days. In addition the specular reflectivity of the Pt(111) terraces is only slightly reduced. At 155 K, the Pt(111)-H (1×1) surface has a reflectivity of about 80% of the clean platinum surface [32].

Besides its superior energy and momentum resolution a He triple-axis spectrometer using microscopic Echelette-gratings features several advantages compared to TOF-spectrometers. In a diffraction scan only the shear elastic intensity is recorded with a crystal spectrometer, no problems from subtracting an inelastic background arise. This is particular advantageous in the study of surface phase transitions. In inelastic experiments a whole variety of new scanning possibilities exists. Each geometrical configuration of a crystal spectrometer corresponds to a single point in the $\hbar\omega - Q$ plane, while in the case of a TOF-spectrometer it corresponds to a parabolic line in the $\hbar\omega - Q$ plane, the scancurve eq. (3). A crystal spectrometer thus features the possibility of constant Q and $\hbar\omega$ scans in addition to the parabolic $\hbar\omega - Q$ scans. In particular the constant Q-scans bear significant advantages in the study of the dispersion and linewidth of surface phonons.

A double surface scattering experiment opens up also fascinating possibilities in the case of molecule (H_2, N_2, etc.) scattering from surfaces. As pointed out by Zare [33] the "double bank shot" is ideally suited for the investigation of the interaction of aligned or oriented molecules with surfaces.

The use of bent crystal surfaces in addition opens up a novel field: molecular beam optics. Indeed, with the feasibility of bending single crystals, metal surfaces can provide the whole spectrum of molecular beam optical elements: mirror-flat fcc (111) surface; focussing mirror-concave fcc (111) surface; dispersive element, beam splitter-flat corrugated surface, e.g., fcc (110)(1×2) reconstructed surfaces; Echelette-grating – regularly stepped metal surface with fcc (111) terraces; focussing Echelette-grating – concave regularly stepped metal surface with fcc (111) terraces.

This spectrum is of great potential use in atomic physics (atom interferometry [34]) as well as in surface science. In the future, one obvious extension would be thermal energy atom microscopy.

Acknowledgement

This contribution is dedicated to George Comsa on the occasion of his 60th birthday. The authors are deeply indebted to George Comsa for his patient and indefatigable guidance during a longer or shorter period of their "scientific" and private life. Without the example, encouragement and criticism of him, the development of the ideas presented in this paper would not have been possible.

References

[1] C.J. Davisson and L.H. Germer, Phys. Rev. 30 (1927) 705.
[2] F. Knauer and O. Stern, Z. Phys. 53 (1929) 779.
[3] T.H. Johnson, Phys. Rev. 37 (1931) 847.
[4] B. Poelsema and G. Comsa, Springer Tracts in Modern Physics 115 (1989) 1.
[5] J.P. Toennies, Springer Series in Surface Science 21 (1991) 111.
[6] K. Kern and G. Comsa, Adv. Chem. Phys. 76 (1989) 211.
[7] B. Poelsema, A.F. Becker, G. Rosenfeld, N. Nagel, L.K. Verheij and G. Comsa, Surf. Sci. 272 (1992) 269.
[8] J.P. Toennies and K. Winkelmann, J. Chem. Phys. 66 (1977) 3965.
[9] R. David, K. Kern, P. Zeppenfeld and G. Comsa, Rev. Sci. Instrum. 57 (1986) 2771.
[10] K. Kern, P. Zeppenfeld, R. David and G. Comsa, J. Vac. Sci. Technol. A 6 (1988) 639.
[11] B. Hall, D.L. Mills, P. Zeppenfeld, K. Kern, U. Becher and G. Comsa, Phys. Rev. B 40 (1989) 6326.
[12] G. Comsa, Surf. Sci. 81 (1979) 57.
[13] K. Kern, P. Zeppenfeld, R. David and G. Comsa, Phys. Rev. B 35 (1987) 886.
[14] P. Zeppenfeld, U. Becher, K. Kern, R. David and G. Comsa, Phys. Rev. B 41 (1990) 8549.
[15] D. Eichenauer, U. Harten, J.P. Toennies and V. Celli, J. Chem. Phys. 86 (1987) 3693.
[16] K. Kern, R. David and G. Comsa, Rev. Sci. Instrum. 56 (1985) 372.
[17] J. Wang, V.A. Shamian, B.R. Thomas, J.M. Wilkinson, J. Riley, C.F. Giese and W.R. Gentry, Phys. Rev. Lett. 60 (1988) 696.
[18] E. Hahn, K. Kuhnke and K. Kern, unpublished.

[19] I. Estermann, O. Frisch and O. Stern, Z. Phys. 73 (1931) 348.
[20] G. Lilienkamp and J.P. Toennies, J. Chem. Phys. 78 (1983) 5210.
[21] B.F. Mason and B.R. Williams, Rev. Sci. Instrum. 49 (1978) 897.
[22] B.F. Mason and B.R. Williams, Phys. Rev. Lett. 46 (1981) 1138.
[23] B. Poelsema, R.L. Palmer, G. Mechtersheimer and G. Comsa, Surf. Sci. 117 (1982) 50;
V. Bortolani, V. Celli, A. Franchini, J. Idiodi, G. Santoro, K. Kern, B. Poelsema and G. Comsa, Surf. Sci. 208 (1989) 1.
[24] G. Comsa, G. Mechtersheimer, B. Poelsema and S. Tomoda, Surf. Sci. 89 (1979) 123.
[25] K. Kuhnke, E. Hahn and K. Kern, unpublished;
Eq. (7) is an approximation which is valid in step down scattering geometry for angles of incidence between 0° and 65°.
[26] A. Guinier, X-ray Diffraction (Freeman, London, 1963).
[27] R.B. Doak, private communication.
[28] E. Hahn, K. Kuhnke and K. Kern, unpublished.
[29] D. Sander, U. Linke and H. Ibach, Surf. Sci. 272 (1992) 318.
[30] F.K. Men, W.E. Packard and M.B. Webb, Phys. Rev. Lett. 61 (1988) 2469.
[31] B. Poelsema, G. Mechtersheimer and G. Comsa, Surf. Sci. 111 (1981) 519.
[32] B. Poelsema, L.S. Brown, K. Lenz, L.K. Verheij and G. Comsa, Surf. Sci. 171 (1986) L395.
[33] R.N. Zare, Z. Phys. D 10 (1988) 377.
[34] D.W. Keith, C.R. Ekstrom, Q.A. Turchette and D.E. Pritchard, Phys. Rev. Lett. 66 (1991) 2693;
O. Carnal and J. Mlynek, Phys. Rev. Lett. 66 (1991) 2689.